

Superconducting State in $\text{SrFe}_{2-x}\text{Co}_x\text{As}_2$ by Internal Doping of the Iron Arsenide Layers

A. Leithe-Jasper, W. Schnelle, C. Geibel, and H. Rosner

Max-Planck-Institut für Chemische Physik fester Stoffe, Nöthnitzer Straße 40, 01187 Dresden, Germany

(Received 15 July 2008; published 14 November 2008)

In the strontium iron-cobalt arsenides $\text{SrFe}_{2-x}\text{Co}_x\text{As}_2$ ($0.2 \leq x \leq 0.4$) superconductivity with T_c up to 20 K is observed in magnetic susceptibility, electrical resistivity, and specific heat data. This first observation of bulk superconductivity induced by electron doping in this family of compounds—despite strong disorder in the Fe-As layer—favors an itinerant electronic theory in contrast to the strongly correlated cuprates and renders a p - or d -wave pairing unlikely. The magnetic ordering present in SrFe_2As_2 is rapidly suppressed by substitution of Fe by Co. Density functional theory calculations show that this is due to a rigid downshift of the Fe- $3d_{x^2-y^2}$ -related band edge in the density of states.

DOI: 10.1103/PhysRevLett.101.207004

PACS numbers: 74.25.Dw, 74.10.+v, 74.25.Bt, 74.25.Fy

This year's discovery of high- T_c superconductivity (HTSC) in layered Fe-As systems has attracted enormous interest. The undoped compounds, e.g., $R\text{FeAsO}$ [1,2] (R = rare-earth element) or $A\text{Fe}_2\text{As}_2$ (A = Ba, Sr) [3–5], present an antiferromagnetic (AFM) ordering related to a structural transition at temperatures in the range 140–205 K. Upon doping both the structural and the magnetic ordering get suppressed and superconductivity with T_c up to 56 K appears [1,6,7]. The onset of HTSC at the disappearance of an AFM ordered state induced by charge doping from a reservoir layer is reminiscent of the behavior observed in the cuprates. Since both Fe and Cu are $3d$ elements, and because of similarities in the structure of the layers, there is a popular claim that there is an analogy between the HTSC in the cuprates and in the layered Fe-As systems. On the other hand, the absence of a Mott-insulator transition as well as the small ordered Fe moment in the undoped compounds suggest that a model based on itinerant and weakly correlated $3d$ electrons might be more appropriate.

One way to get insight into the superconducting mechanism is a doping experiment on the Fe site. Presently, doping is only performed on sites in-between the Fe-As layers, either on the R or the O site in $R\text{FeAsO}$ systems or on the A site in $A\text{Fe}_2\text{As}_2$ compounds. Such kind of doping corresponds, both in a localized and in an itinerant model, to a simple charge doping and is therefore not suitable for discriminating between both models. In an itinerant model, within a simple rigid-band approach, the substitution of a small amount of Fe by another $3d$ element is expected to be similar to indirect doping via interlayer sites since only the total count of electrons is relevant. In a picture with localized $3d$ electrons, doping on the Fe site should lead to a drastically different behavior since correlations in the $3d$ layers are directly affected. For example, a few percent Ni or Zn substitution on the Cu site in a HTSC cuprate leads to a drastic reduction of T_c .

Therefore, we investigated the properties of the solid solution $\text{SrFe}_{2-x}\text{Co}_x\text{As}_2$. While pure SrFe_2As_2 undergoes

a lattice distortion and AFM ordering at $T_0 = 205$ K [4], a small amount of Co substitution leads to a rapid decrease of T_0 , followed by the onset of bulk superconductivity in the concentration range $0.2 \leq x \leq 0.4$ with a maximum T_c of ≈ 20 K. This is the first observation of electron-doping induced superconductivity in $A\text{Fe}_2\text{As}_2$ compounds. The appearance of superconductivity due to in-plane Co doping *per se* provides strong evidence that an analogy with the HTSC cuprates is not justified. We thus performed band structure calculations and discuss the electronic structure in view of our experimental results and conclude that an itinerant approach is appropriate for these layered Fe-As systems. The observation of superconductivity despite large in-layer disorder puts also a strong constraint on the possible superconducting order parameter. While finalizing our investigation, Sefat *et al.* [8] and Wang *et al.* [9] reported superconductivity in Co doped LaFeAsO with a maximum $T_c \approx 10$ K. While their results support our analysis, the higher T_c found in $\text{SrFe}_{2-x}\text{Co}_x\text{As}_2$ establishes a stronger evidence.

Samples were prepared by sintering in glassy-carbon crucibles which were welded into tantalum containers and sealed into evacuated quartz tubes for heat treatment at 900 °C for 16 h with two regrinding and compaction steps. First, precursors SrAs , Co_2As and Fe_2As were synthesized from elemental powders sintered at 600 °C for 48 h (Fe, Co 99.9 wt. %; As 99.999 wt. %; Sr 99.99 wt. %). The usage of these precursors minimizes the content of elemental As [10] and ferromagnetic (Fe) impurities. These educts were powdered, blended in stoichiometric ratios, compacted to pellets, and heat treated. All sample handling was done inside argon-filled glove boxes.

Metallographic preparations and optical microstructure investigation were performed on polished surfaces. Electron-probe microanalysis (EPMA) with energy dispersive analysis was accomplished in a Philips XL30 scanning electron microscope. Powder x-ray diffraction was performed using Co $K\alpha 1$ radiation ($\lambda = 1.789007$ Å) applying the Guinier Huber technique with LaB_6 as internal

standard ($a = 4.15692 \text{ \AA}$). Crystallographic calculations were done with the WINCSD program package [11].

Evaluation of the lattice parameters and EPMA investigations of the samples confirm the nominal stoichiometry and confirm the substitution of Fe by Co which is accompanied by a decrease of the c axis length of the unit cell (see Table I). For the sample $\text{SrFe}_{1.8}\text{Co}_{0.2}\text{As}_2$ which was essentially single phase (minor impurity SrAs) the crystal structure was refined by Rietveld methods (BaAl₄-type structure [12], space group $I4/mmm$, Sr in $2a$ (0, 0, 0), Fe/Co in $4d$ (0, 1/2, 1/4), As in $4e$ (0, 0, 0.3613(1)); $R_I = 7.4$, $R_P = 10.1$). Other samples contained minor patches (<1%) of $\text{Fe}_{1-x}\text{Co}_x\text{As}$ phases. No indication for a structural ordering of the Co was found.

Magnetization was measured from 1.8–400 K in a SQUID magnetometer in various fields both after zero-field cooling (ZFC) and during cooling in field (FC). Heat capacity was determined by a relaxation-type method on a commercial measurement system (1.9–100 K, 0–9 T). Electrical dc resistivity data $\rho(T)$ (3.8–320 K) were collected with a current density of $<1 \times 10^{-3} \text{ A mm}^{-2}$ in a four contact arrangement.

To investigate the influence of electron doping on the electronic structure of SrFe_2As_2 on a microscopic level, we performed density functional band structure calculations within the local (spin) density approximation [L(S)DA]. Using the experimental structural parameters [4], we applied the full-potential local-orbital code FPLO [13] (version 7.00–28) with the Perdew-Wang exchange correlation potential and a carefully converged k -mesh of 24^3 points for the Brillouin zone. The substitution of Fe by Co and Sr by La was simulated within the virtual crystal approximation (VCA).

The magnetic susceptibility in a nominal field $\mu_0 H = 2 \text{ mT}$ (Fig. 1 top) displays strong diamagnetic signals in ZFC due to superconducting transitions in the $x = 0.2$ – 0.4 samples with onset temperatures T_c^{mag} up to 19.2 K (see Table I). The compounds with $x = 0.1$ and $x = 0.5$ show

TABLE I. Lattice parameters a , c of $\text{SrFe}_{2-x}\text{Co}_x\text{As}_2$ (nominal compositions) and superconducting transition temperature T_c^{mag} (crossing of the tangent to the steepest slope of the FC transition with $\chi = 0$, $T_{\text{min}} = 1.8 \text{ K}$), χ_0 is the high-field susceptibility extrapolated to $T = 0$. (\dots) = traces of ferromagnetic impurities, e.g., iron metal. Data for $x = 0$ are from Ref. [4].

x	a (\AA)	c (\AA)	T_c^{mag} (K)	χ_0 (10^{-6} emu/mol)
0.00	3.924(3)	12.34(1)		\dots
0.10	3.9291(1)	12.3321(7)		\dots
0.15	3.9272(1)	12.3123(5)		+780
0.20	3.9278(2)	12.3026(2)	19.2	+600
0.25	3.9296(2)	12.2925(9)	18.1	+850
0.30	3.9291(2)	12.2704(8)	13.2	+460
0.40	3.9293(1)	12.2711(7)	12.9	+360
0.50	3.9287(2)	12.2187(9)		\dots
1.00	3.9618(1)	11.6378(6)		\dots

no traces of superconductivity for $T > 1.8 \text{ K}$. The transitions are rounded indicating that the samples are not fully homogeneous. While the shielding signal (ZFC) corresponds to the whole sample volume, the Meissner effect (FC) is very small which is likely due to strong pinning induced by the random substitution of Fe by Co within the superconducting layers.

The susceptibilities of the samples $x = 0.2, 0.3$, and 0.4 are field independent for $T > 200 \text{ K}$. There, they display a paramagnetism which can be described by $\chi(T) = \chi_0 + \chi_2 T^2$. Such extrapolated χ_0 values are given in Table I (core contributions are only $\approx -50 \times 10^{-6} \text{ emu/mol}$). Although the current sample quality does not allow for a detailed analysis of χ_0 , its order of magnitude and temperature dependence ($\propto T^2$) are typical for an enhanced Pauli paramagnet. Comparing the χ_0 values with the electronic density of states (DOS) at the Fermi level ε_F obtained from band structure calculations (see below) suggests an enhanced Sommerfeld-Wilson ratio, which decreases with increasing Co content for $x \geq 0.15$, in accordance with a magnetic instability for $x \leq 0.15$. SrCo_2As_2 is a Curie-Weiss paramagnet ($\mu_{\text{eff}} = 2.06 \mu_B/\text{f.u.}$, $\theta_{\text{CW}} = -29 \text{ K}$) and does not order magnetically above 1.8 K.

The temperature dependence of the resistivity $\rho(T)$ (Fig. 1 bottom) at high T is generally metallic. $\rho(300 \text{ K})$ decreases gradually with electron doping from $8 \mu\Omega \text{ m}$ for $x = 0.15$ to $2 \mu\Omega \text{ m}$ for $x = 0.50$, as also observed for potassium substituted samples [3]. For $x = 0.10$ a steplike increase of $\rho(T)$ is observed below $\approx 130 \text{ K}$. This step shifts to $\approx 90 \text{ K}$ for $x = 0.15$. This anomaly can be as-

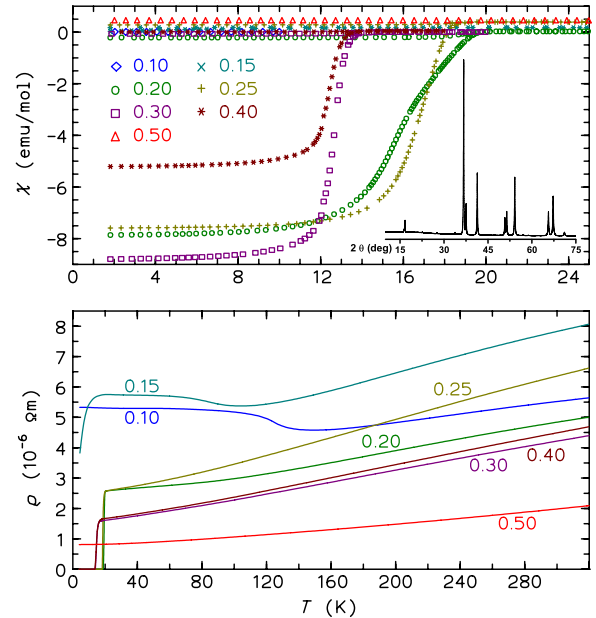


FIG. 1 (color online). Top: magnetic susceptibility $\chi(T)$ of $\text{SrFe}_{2-x}\text{Co}_x\text{As}_2$ samples in a nominal field of $\mu_0 H = 2 \text{ mT}$. The inset shows the x-ray diffraction pattern of the $x = 0.2$ sample. Bottom: electrical resistivity of the same samples.

signed to the AFM ordering and the related lattice distortion observed at $T_0 = 205$ K in SrFe_2As_2 [4,5]. Thus, Co substitution (electron doping) leads to the suppression of the AFM order in a similar way as reported for K substitution (hole doping) [14]. For $x = 0.20$ no such anomaly is seen and the compound exhibits a superconducting transition at 19.4 K. A tentative experimental phase diagram is given in the inset of Fig. 2.

In Fig. 2 the specific heat $c_p(T)$ for two selected samples is presented in a $c_p(T)/T^2$ versus T plot. Rounded anomalies with onset at T_c as determined by $\rho(T)$ and $\chi(T)$ data are visible. Hence, superconductivity is a bulk phenomenon in these samples. The idealized step heights Δc_p and the transition temperatures T_c^{cal} were evaluated by a fit with a phononic background and an electronic term according to the BCS theory ($\Delta c_p/T_c = 1.43\gamma$) or the two-liquid model ($\Delta c_p/T_c = 2\gamma$) which approximates the thermodynamics of some strong coupling superconductors. The models are convoluted with a Gaussian to simulate the broadening. We obtain $\Delta c_p/T_c^{\text{cal}} \approx 10 \text{ mJ mol}^{-1} \text{ K}^{-2}$ for $x = 0.2$ and $\approx 13 \text{ mJ mol}^{-1} \text{ K}^{-2}$ for $x = 0.3$. Interestingly, well below T_c the specific heat can still be described by a linear plus a T^3 Debye lattice term, i.e., $c_p(T) = \gamma'T + \beta T^3$. While β is field-independent with an initial Debye temperature $\Theta_D(0) = 255(2)$ K for both samples $x = 0.2$ and 0.3 , the linear coefficient γ' increases nearly linearly with field. For $x = 0.2$ the values of γ' range from $12.6 \text{ mJ mol}^{-1} \text{ K}^{-2}$ at $\mu_0 H = 0 \text{ T}$ to $17.5 \text{ mJ mol}^{-1} \text{ K}^{-2}$ at 9 T. Whether the residual γ' is induced by defects (see, e.g., Ref. [15]) or whether it is an intrinsic contribution due to ungapped parts

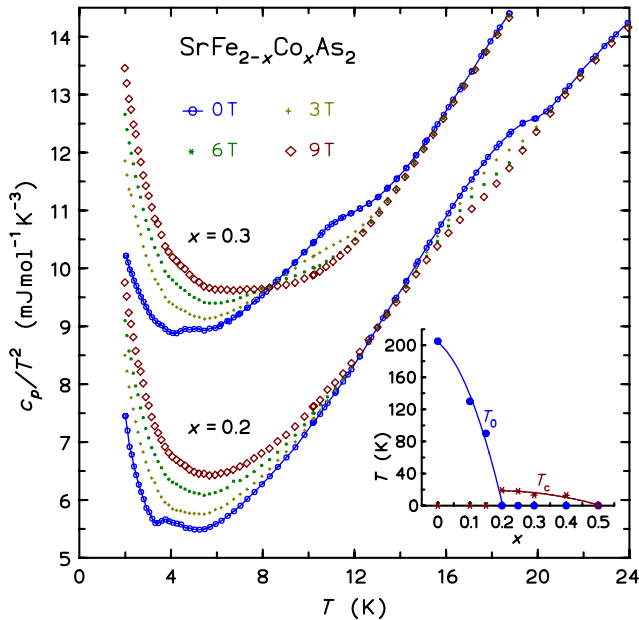


FIG. 2 (color online). Molar isobaric specific heat $c_p(T)/T^2$ of $\text{SrFe}_{2-x}\text{Co}_x\text{As}_2$ samples ($x = 0.2$; $x = 0.3$ shifted up by 3 units) for different magnetic fields. Data for $\mu_0 H = 0$ are connected by a line. The inset shows the transition temperatures T_0 and T_c versus Co content x .

of the Fermi surface [16] has to be elucidated by further experiments. For $x = 0.2$ the best fit is obtained within the two-fluid model. In contrast, the BCS fit is superior for $x = 0.3$. This might indicate a variation of the coupling strength with Co content.

For a microscopic study of the influence of doping with electrons on the electronic structure in the vicinity of the Fermi level ε_F , we simulated two kinds of partial constituent exchange: (i) Co substitution at the Fe site and (ii) a fictitious La substitution at the Sr site to study possible differences for doping (i) within and (ii) outside the FeAs layers. Throughout all calculations we used the experimental lattice parameters [4] of SrFe_2As_2 to separate the influence of geometry changes and pure electronic doping effects. Since the changes of the lattice parameters upon doping are very small (see Table I) this approach is justified. The resulting total DOS for the Fe-3d dominated regions of the valence band for $\text{SrFe}_{2-x}\text{Co}_x\text{As}_2$ and $\text{Sr}_{1-x}\text{La}_x\text{Fe}_2\text{As}_2$, respectively, is shown in Fig. 3 for an exemplary doping level of $x = 0.3$.

The two kinds of doping result in a rather different behavior. Whereas (i) Co substitution leads to an almost perfectly rigid shift of the DOS for all studied doping levels between $x = 0$ and $x = 0.5$, (ii) La substitution cannot be described at all in a rigid-band picture in the vicinity of ε_F (Fig. 3). In case of Co substitution (i), an analysis of the orbital-resolved DOS, the corresponding bands and band characters show that the rigid-band picture holds even for the individual orbitals close to ε_F . In contrast, La substitution (ii) shifts down the energy and changes the dispersion of a band with Fe-As-Sr hybrid character in a way that it gets partially occupied, whereas other bands remain basically unchanged. In consequence, this leads to the formation of a pronounced peak at ε_F and a sizable increase of the DOS (Fig. 3). In general, from the experimental results for $R\text{FeAsO}$ and $A\text{Fe}_2\text{As}_2$ compounds, it

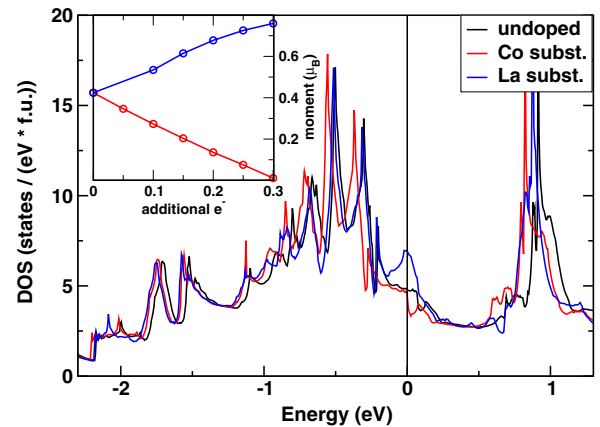


FIG. 3 (color online). Total electronic densities of states for SrFe_2As_2 (black), $\text{SrFe}_{1.7}\text{Co}_{0.3}\text{As}_2$ (red or gray) and for the fictitious $\text{Sr}_{0.7}\text{La}_{0.3}\text{Fe}_2\text{As}_2$ (blue or dark gray) in the vicinity of the Fermi level. Inset: dependence of the magnetic moment on the number of additionally doped electrons per formula unit for doping at the Fe site (red) and at the Sr site (blue), respectively.

seems that the appearance of bulk HTSC is intrinsically related to the prior destruction of the spin density wave. Therefore, we studied the instability towards magnetism depending on the doping level for scenarios (i) and (ii). In Fig. 3 (inset) we plot the size of the ordered Fe moment corresponding to the minimum in total energy obtained by VCA-LSDA calculations as a function of substitution. (ii) While La substitution stabilizes the magnetic state, (i) electron doping by Co leads to the disappearance of the magnetic state at $x = 0.3$.

The disappearance of the magnetic instability is intimately related to the occupation of the Fe- $3d_{x^2-y^2}$ related band along the Γ -Z direction as previously demonstrated [4] for the undoped compound (depending on the As z position). For $x = 0.3$ (see Fig. 3) the related band edge is situated right at ε_F , leading to a reduced DOS and thus to the destruction of the magnetic state. In contrast, the tendency towards magnetism would be increased for (ii) La substitution. The DOS enhancement upon La substitution might lead to an instability of the $\text{Sr}_{1-x}\text{La}_x\text{Fe}_2\text{As}_2$ phase, which could be the reason why such compositions have not yet been reported.

The nonmagnetic state in the VCA-LSDA calculations for $\text{SrFe}_{2-x}\text{Co}_x\text{As}_2$ with $x \leq 0.3$ is in surprisingly good agreement with the experimentally observed disappearance of the magnetic state and the onset of superconductivity for $x = 0.2$. In fact, the used VCA should result in an overestimate of the stability of a magnetic ground state since it does not include the direct influence of disorder inside the Fe-As layer. Most likely, the Co impurities are nonmagnetic, as indicated by calculations for SrCo_2As_2 that yield a nonmagnetic ground state in agreement with our measurements. Thus, a more sophisticated treatment of the Co impurities should lead to a sizable reduction of the critical concentration x for the suppression of the magnetic instability, in line with our experiments.

In summary, with the $\text{SrFe}_{2-x}\text{Co}_x\text{As}_2$ series we investigated how electron doping within the Fe-As layers affects the magnetic and electronic properties. We found that Co substitution rapidly suppresses the AFM transition and the associated lattice distortion. For $x = 0.2$, AFM order is destroyed and bulk superconductivity with a $T_c \approx 20$ K appears. Higher Co content leads to a reduction of T_c and finally to the disappearance of superconductivity for $x \approx 0.5$. Thus electron doping within the Fe-As layer by substituting Co for Fe has a similar effect as hole doping in between the layers by substituting K for Sr.

The observation of superconductivity upon substitution on the $3d$ site in the layered Fe-As systems is in strong contrast to the behavior in the cuprates, where substitution on the Cu site lead to a fast suppression of superconductivity. This indicates that the suggested analogy of HTSC in cuprates and in Fe-As systems is not appropriate. Instead we observe a rigid-band-like shift of the DOS to lower

energy upon Co substitution. Indeed, a sample of composition $\text{SrFe}_{1.9}\text{Ni}_{0.1}\text{As}_2$ (doping with $0.2 e^-$) shows superconductivity at ≈ 8 K. The suppression of the magnetic state, which occurs in the calculations at $x = 0.3$, is related to the $d_{x^2-y^2}$ states being pushed below the Fermi level. In contrast, our calculations show that electron doping by substituting La for Sr leads to a change in the dispersion and energy of a Fe-As-Sr hybrid band. The resulting increase of the DOS at ε_F stabilizes the magnetic state and might induce an instability of the SrFe_2As_2 phase. The correspondence between the experiments and VCA-LSDA band structure calculations indicates that an approach based upon itinerant, weakly correlated $3d$ electrons is more appropriate for the description of the Fe-As systems than a picture relying on localized $3d$ moments.

We thank U. Burkhardt, T. Vogel, R. Koban, K. Kreutziger, Yu. Prots, and R. Gumeniuk for assistance.

Note added.—A similar report on superconductivity at 22 K in Co-substituted BaFe_2As_2 was published recently in this journal [17].

-
- [1] Y. Kamihara, T. Watanabe, M. Hirano, and H. Hosono, *J. Am. Chem. Soc.* **130**, 3296 (2008).
 - [2] C. de la Cruz *et al.*, *Nature (London)* **453**, 899 (2008).
 - [3] M. Rotter, M. Tegel, I. Schellenberg, W. Hermes, R. Pöttgen, and D. Johrendt, *Phys. Rev. B* **78**, 020503 (R) (2008).
 - [4] C. Krellner, N. Caroca-Canales, A. Jesche, H. Rosner, A. Ormeci, and C. Geibel, *Phys. Rev. B* **78**, 100504(R) (2008).
 - [5] M. Tegel, M. Rotter, V. Weiss, F.M. Schappacher, R. Pöttgen, and D. Johrendt, arXiv:0806.4782v2.
 - [6] C. Wang *et al.*, *Europhys. Lett.* **83**, 67006 (2008).
 - [7] M. Rotter, M. Tegel, and D. Johrendt, *Phys. Rev. Lett.* **101**, 107006 (2008).
 - [8] A. S. Sefat *et al.*, *Phys. Rev. B* **78**, 104505 (2008).
 - [9] C. Wang *et al.*, arXiv:0807.1304v2.
 - [10] J.O. Nriagu, *Arsenic in the Environment, Human Health and Ecosystem Effects* (Wiley, New York, 1994), Pt. II.
 - [11] L.G. Akselrud, P.Y. Zavalii, Yu. Grin, V.K. Pecharsky, B. Baumgartner, and E. Wölfel, *Mater. Sci. Forum* **133–136**, 335 (1993).
 - [12] K.R. Andress and E. Alberti, *Z. Metallkd.* **27**, 126 (1935).
 - [13] K. Koepf and H. Eschrig, *Phys. Rev. B* **59**, 1743 (1999).
 - [14] G.F. Chen *et al.*, *Chin. Phys. Lett.* **25**, 3403 (2008).
 - [15] G. Triscone and A. Junod, in *Bismuth-Based High-Temperature Superconductors*, edited by H. Maeda and K. Togano (Marcel Dekker, New York, 1996), pp. 33–74.
 - [16] S.L. Drechsler *et al.*, *Physica (Amsterdam)* **B329**, 1352 (2003).
 - [17] A. S. Sefat, R. Jin, M.A. McGuire, B.C. Sales, D.J. Singh, and D. Mandrus, *Phys. Rev. Lett.* **101**, 117004 (2008).